

1 **Utilization of guaiacol-based deep eutectic solvent for achieving a**  
2 **sustainable biorefinery**

3 Chen Huang<sup>1,2,3</sup>, Jinyuan Cheng<sup>1</sup>, Yunni Zhan<sup>1</sup>, Xuze Liu<sup>1</sup>, Jia Wang<sup>2</sup>, Yunxuan Wang<sup>6</sup>,  
4 Chang Geun Yoo<sup>6</sup>, Guigan Fang<sup>1</sup>, Xianzhi Meng<sup>3,\*</sup>, Arthur J. Ragauskas<sup>3,4,5</sup>, Xueping Song<sup>7</sup>

5 <sup>1</sup>Institute of Chemical Industry of Forest Products, Chinese Academy of Forestry, Jiangsu  
6 Province Key Laboratory of Biomass Energy and Materials, Nanjing 210042

7 <sup>2</sup>Co-Innovation Center for Efficient Processing and Utilization of Forest Resources, Nanjing  
8 Forestry University, Nanjing 210037, China

9 <sup>3</sup>Department of Chemical and Biomolecular Engineering, University of Tennessee Knoxville,  
10 Knoxville, TN 37996, USA

11 <sup>4</sup>Department of Forestry, Wildlife, and Fisheries, Center for Renewable Carbon, The  
12 University of Tennessee Institute of Agriculture, Knoxville, TN 37996, USA

13 <sup>5</sup>UTK-ORNL Joint Institute for Biological Science, Biosciences Division, Oak Ridge National  
14 Laboratory, Oak Ridge, TN 37831, USA

15 <sup>6</sup>Department of Paper and Bioprocess Engineering, State University of New York College of  
16 Environmental Science and Forestry, Syracuse, NY 13210-2781, USA.

17 <sup>7</sup>Guangxi Key Laboratory of Clean Pulp & Papermaking and Pollution Control, College of  
18 Light Industry and Food Engineering, Guangxi University, Nanning 530004, China

19 **Abstract**

20 This study proposed a renewable deep eutectic solvent (DES) pretreatment using lignin-  
21 derived guaiacol as the hydrogen bond donor. The DES showed excellent biomass

22 fractionation efficiency after the incorporation of trace  $\text{AlCl}_3$  as the reinforcer, which removed  
23 79.1% lignin while preserving more than 90% glucan. The pretreated bamboo exhibited 96.2%  
24 glucan enzymatic hydrolysis yield at only 110 °C. The physicochemical properties of the  
25 pretreated solids were comprehensively investigated to explain how the DES fractionation  
26 overcame the biomass recalcitrance. The regenerated lignin from the DES pretreatment was  
27 also analyzed, which revealed that lignin  $\beta$ -O-4 bond was significantly cleaved. This guaiacol-  
28 based DES could greatly contribute to establish a closed-loop biorefinery sequence with high  
29 lignin fractionation efficiency and great solvent recyclability.

30 *Keywords: guaiacol, DES, lignin, enzymatic hydrolysis*

## 31 **1. Introduction**

32 Lignocellulose refining into fuels and chemicals is deemed as an ideal substitute for the  
33 petroleum refinery because the petroleum is not sustainable and is depleting quickly  
34 (Ragauskas et al., 2006). Lignocellulosic biomass has a rigid and compact structure, and its  
35 carbohydrate polymers such as cellulose and hemicellulose are tightly bound to lignin through  
36 various chemical linkages. This inherent nature restricts various type of biomass processing  
37 such as enzymatic hydrolysis, calling for a pretreatment technology to separate the main  
38 components for their individual valorization. In past decades, numerous pretreatment methods  
39 have been developed, such as acid pretreatment, alkaline pretreatment, hydrothermal, steam  
40 explosion pretreatment, organosolv pretreatment, and so on (Alayont et al., 2022; Zhan et al.,  
41 2022).

42           Unfortunately, none of these technologies led to a successful industrial application due to  
43 their inevitable drawbacks. For example, acid pretreatment could cause excessive degradation  
44 of hemicellulose, generate fermentation inhibitors and corrode the equipment (Liu et al.,  
45 2019); while alkaline pretreatment is disadvantageous in the aspects of high downstream  
46 processing cost and generation of phenolic inhibitors (Carvalho et al., 2016).

47           In traditional carbohydrate-centered biorefinery, the major objective of the pretreatment is  
48 to recover digestible cellulose-rich substrate. In this vein, lignin as the most recalcitrant  
49 biomass components needs to be removed or redistributed from the plant cell wall (Studer et  
50 al., 2011). Typical industrialized lignin-target pretreatments mainly include kraft pulping and  
51 alkaline peroxide bleaching. Kraft pulping is typically accomplished at elevated temperatures  
52 and high pressure to digest wood chips and extract lignin from the cell wall in a water solution  
53 of sodium sulfide and sodium hydroxide. During the process, lignin suffers from irreversible  
54 degradation as well as severe condensation reactions that are detrimental to further processing.  
55 As to the alkaline peroxide bleaching which is normally carried out at much mild temperature  
56 (*e.g.*, 90-100 °C), highly reactive hydroxyl radical (HO·) and superoxide anion radical (O<sub>2</sub><sup>·-</sup>)  
57 are generated to oxidize the lignin macromolecule, causing the cleavage of side chain and  
58 depolymerizing the lignin (Ho et al., 2019). Unfortunately, the solubilized lignin further  
59 undergoes a ring-opening reaction to generate organic acid, which makes it hard to recover.

60           To make the lignocellulose biorefinery profitable, the efficient co-conversion or  
61 utilization of cellulose and lignin becomes necessary. Considering the fact that lignin inhibits  
62 cellulose digestibility, the removal of lignin will inevitably increase the cellulose

63 accessibility/digestibility. Lignin is the most abundant aromatic compound on earth, and it has  
64 the potential to be processed into diverse products, ranging from jet fuel to dispersant, glue,  
65 resins, and nanocomposites. However, lignin depolymerization and condensation reaction  
66 during these delignification pretreatments hampered its valorization potential, and a multitude  
67 of work has been proposed aiming to preserve the native lignin structure. Generally, there is a  
68 trade-off between the lignin structural integrity and its recovery yield as the extent of aryl ether  
69 preservation heavily depends on the pretreatment severity. For example, high pretreatment  
70 severity typically leads to high delignification efficiency but low lignin structure integrity. In  
71 recent years, Luterbacher and co-workers found that the existence of formaldehyde could  
72 effectively suppress the lignin condensation by forming stable acetals at the  $\alpha$ -OH and  $\beta$ -OH of  
73 lignin's side chain, resulting in a close-to-theoretical monomer yield after hydrogenolysis  
74 (Bueren et al., 2020; Shuai et al., 2016). Thereafter, other chemicals such as 1,4-butanediol and  
75 2-naphthol were also found to be capable of reducing the condensation and preserving the aryl  
76 ether of lignin (Cheng et al., 2022; Pielhop et al., 2015). In addition to obtaining the high aryl  
77 ether content lignin, other researchers reported that lignin could be isolated and self-assembled  
78 into nanospheres after organosolv pretreatment, while the residual solid showing more than  
79 90% digestibility after enzymatic hydrolysis (Liu et al., 2019).

80 Deep eutectic solvent (DES), a green alternative solvent to ionic liquid, has attracted  
81 much attention as it possesses almost all the advantages of ionic liquid while it is environment  
82 friendly, renewable, non-toxic, and biocompatible. Generally, DES is composed of hydrogen  
83 bond acceptors (HBA, *e.g.*, choline chloride) and hydrogen bond donors (HBD), which could

84 compete with the inner hydrogen bond in biomass and cause its fractionation. Interestingly,  
85 DES is reported to be able to selectively extract the lignin, making it a preferential solvent for  
86 the preparation of technical lignins. However, most of the literatures concerning DES used  
87 organic acids and alcohols as HBD, and the investigation of using renewable solvent in DES  
88 synthesis is still in its infancy. There is a trend in using biomass-derived compounds to  
89 synthesize the DES, which could benefit the constitution of a closed-loop biorefinery (Wang et  
90 al., 2020). Guaiacyl is one of the key basic units in lignin, and many studies have prepared  
91 guaiacol through lignin catalytic depolymerization (Shen et al., 2020). Here in this study,  
92 guaiacol was used as the HBD to synthesize a DES system that showed excellent  
93 delignification efficiency and high biomass digestibility after pretreatment. After the guaiacol-  
94 DES pretreatment, the lignin could be used for the preparation of guaiacol, which could  
95 establish a close-loop biorefinery sequence. Till now, very limited work was conducted using  
96 lignin-derived chemicals for DES synthesis and application in biomass process. Thus, the  
97 utilization of guaiacol-DES for biomass fractionation may offer a guide in establishing lignin-  
98 based DES pretreatment and further help to achieve a green and sustainable biorefinery  
99 configuration.

## 100 **2. Materials and Methods**

### 101 2.1. Materials

102 Moso bamboo (*Phyllostachys edulis*) was provided by a pulp mill (Xianhe Co., Ltd) in  
103 Zhejiang Province, China. The bamboo culms were first mechanically treated to disintegrate  
104 the bamboo culms and generate bamboo fibrils, and the details can be found in a previous

105 study (Zhan et al., 2022). The bamboo fibrils were then air-dried at room temperature until the  
106 moisture content was less than 10% and stored in the dark prior to DES pretreatment. Choline  
107 chloride (ChCl), guaiacol, and anhydrous aluminum chloride ( $\text{AlCl}_3$ ) were purchased from  
108 Macklin Biochemical Co., Ltd (Shanghai, China). All other chemicals of analytical grade were  
109 obtained from Sinopharm Chemicals reagents (Beijing, China) and were used without further  
110 purification.

## 111 2.2. DES preparation and pretreatment

112 The DES was prepared according to the previous research, in which ChCl, guaiacol, and  
113  $\text{AlCl}_3$  (molar ratio of 25:50:1, any changes of the molar ratio are illustrated in the content)  
114 were weighed into a three-neck flask at 80 °C to form a homogeneous and transparent liquid  
115 (Huang et al., 2021). The DES was stored in a desiccator at room temperature until use.

116 The DES pretreatment was conducted at a 1:10 (wt/wt) biomass-to-DES ratio in the three-  
117 neck flasks. In detail, 10 g dried bamboo was mixed with 100 g of DES in a beaker, which was  
118 then transferred into a 250 mL three-neck flask. The flasks containing bamboo and DES were  
119 placed in the preheated oil bath with agitation at temperature of 80-150 °C, and maintained at  
120 the temperature for 60 min. After the pretreatment, the slurry was poured into 500 mL anti-  
121 solvent (50 v/v% acetone/water) and stirred at room temperature for 1 h to quench the reaction.  
122 The solid and liquid were then separated with vacuum filtration, and the filter cake was further  
123 rinsed with deionized water and then stored at 4 °C. The liquid was subjected to rotary  
124 evaporation at 50 °C to remove the acetone, after which it was added with 400 mL of  
125 deionized water to precipitate the lignin (Huang et al., 2022). The precipitated lignin was

126 finally obtained by centrifugation and was defined as DES lignin. The residual liquid after  
127 lignin recovery was rotary evaporated at 70 °C to remove the water and recover the DES for  
128 next round of pretreatment.

### 129 2.3. Analytical procedures

130 Enzymatic hydrolysis (EH) was conducted in 100 mL glass flasks with a solid loading of  
131 2.5% and a working volume of 20 mL. The cellulase and xylanase were added at the dosages  
132 of 25 FPU/g glucan and 150 U/g xylan, respectively. The flasks were incubated at 50 °C and  
133 150 rpm for 72 h. EH yield was calculated using the following equation:

$$134 \quad \text{EH yield (\%)} = \frac{\text{glucose/xylose in the enzymatic hydrolyzate (g)}}{\text{initial glucose/xylose in the substrate (g)}} \times 100\%$$

135 The chemical compositions of all the samples in this study were analyzed according to the  
136 NREL standard (Sluiter et al., 2008). All the monomeric sugars in this study were quantified  
137 with an Agilent HPLC (Agilent 1260 II, Agilent Technologies).

138 The surface morphology of the samples was observed with a Hitachi scanning electron  
139 microscopy (SEM, 3400-I, Hitachi, Japan) at the voltage of 15 kV. XRD spectra (X-ray  
140 diffraction) were recorded with a Bruker D8 advanced instrument (Bruker, Germany). The  
141 instrument used Cu K $\alpha$  radiation as the X-ray source at the voltage of 40 kV and current of 30  
142 mA over the 2 $\theta$  range of 10-40°. FTIR spectra were obtained with an ATR-FTIR spectrometer  
143 (is10, Thermo Nicolet Corporation, USA) in transmittance mode over the wavenumber range  
144 of 4000-500 cm<sup>-1</sup>.

145 Cellulose degree of polymerization (DP) was measured according to the capillary  
146 viscometry procedure (Buzala et al., 2017). First, the holocellulose was obtained by

147 delignifying samples in acid sodium chlorite solution for 4 h, during which fresh sodium  
148 chlorite and acetic acid were added every hour (Cheng et al., 2022). After that, 1.00 g of the  
149 holocellulose was added into 50 mL 17.50 w/v% NaOH solution and stirred for 2 h at RT.  
150 After that, another 50 mL of deionized water was added to dilute the NaOH solution to 8.75  
151 w/v% and stirred for an additional 2 h to remove the hemicellulose. Finally, the solid residue  
152 (*i.e.*,  $\alpha$ -cellulose) was obtained by centrifuging the alkaline slurry and washing with 100 mL of  
153 1 wt% acetic acid, and then rinsed with excessive deionized water. 0.10 g of the obtained dry  
154  $\alpha$ -cellulose (freeze-dried) was dissolved in 20 mL of 0.50 M cupriethylenediamine solution,  
155 and the cellulose solution was subjected to a capillary viscometer in a 25 °C water bath.

156 Cellulose DP was calculated using the following equation:

$$157 \quad DP=0.75 \times [954 \times \log X - 325]$$

158 Where X is the determined viscosity of the generated mixture.

#### 159 2.4. Lignin structure analysis

160 Cellulolytic enzyme lignin (CEL) was isolated from the raw bamboo according to a  
161 previous study (Meng et al., 2017). The weight-average ( $M_w$ ) and number-average ( $M_n$ )  
162 molecular weights of the acetylated CEL and DES lignins were determined by a Waters GPC  
163 (gel permeation chromatography, Waters 2489, Waters, USA). The chemical structure of the  
164 lignins in this study was analyzed by HSQC (heteronuclear single quantum coherence) NMR  
165 (nuclear magnetic resonance). The lignin sample was first dissolved in DMSO- $d_6$  and the  
166 NMR spectra were acquired by a Bruker Ascend™ 600 MHz NMR spectrometer. A standard  
167 Bruker heteronuclear quantum coherence pulse sequence on a 5 mm  $N_2$  cryogenically cooled

168 Broadband Observe (BBO) H&F probe was used with the following conditions: 12 ppm  
169 spectral width in F2 (1H) dimension with 1024 data points and 166 ppm spectral width in F1  
170 (<sup>13</sup>C) dimension with 256 data points, a 1.0 s pulse delay, a J<sub>C-H</sub> of 145 Hz, and 128 scans.

### 171 **3. Results and discussion**

#### 172 3.1. Composition analysis

173 Prior to this study, various pretreatments (*e.g.*, autohydrolysis and alkaline peroxide) have  
174 been conducted on moso bamboo, and results showed that relatively low sugar release was  
175 achieved during enzymatic hydrolysis process when compared to that using other bamboo  
176 species (*Neosinocalamus affinis*) as starting materials (Zhan et al., 2022). This indicated that  
177 moso bamboo was a much more recalcitrant biomass than other types of bamboo species.

178 Other researchers also observed a similar phenomenon, and they ascribed it to the complicated  
179 chemical structure of moso bamboo, including higher lignin molecular weight and high content  
180 of the lignin-carbohydrate complex (Wen et al., 2015). In this study, a novel guaiacol-based  
181 DES pretreatment was performed on the moso bamboo with an objective to recover the high-  
182 quality lignin and facilitate the enzymatic hydrolysis of the residual cellulose-enriched solid.  
183 The effects of the pretreatment temperature on the solid recovery and compositional analysis  
184 are shown in Fig. 1. As shown, the solid yield decreased gradually from 89.18% to 77.40%,  
185 65.37%, 57.16%, and 53.12% as the temperature increased from 80 to 120 °C, indicating more  
186 biomass components were dissolved at high temperature. However, when the temperature  
187 exceeded 120 °C, solid yield started to increase and finally reached 70.68% at 150 °C. The  
188 detailed composition recovery as shown in Fig. 1b could be used to explain the trend of the

189 solid recovery. The glucan was observed to be very stable during the proposed DES  
190 pretreatment with its recovery remaining >90% (90.95%-96.32%). This result is consistent  
191 with a previous study showing that very limited amount of cellulose was degraded during the  
192 DES pretreatment (Shen et al., 2019). Unlike cellulose, DES pretreatment was proved to be  
193 much more selective for xylan and lignin removal especially at higher temperatures. For  
194 example, at a low temperature of 80 °C, 77.77% xylan could be recovered, and the xylan  
195 degradation was much more pronounced with increasing temperature, especially at the  
196 temperature higher than 100 °C. Finally, only 4%-5% of xylan was recovered at 120-150 °C,  
197 indicating that xylan suffered from significant degradation during the proposed DES  
198 pretreatment. The removal of lignin also significantly increased from 16.30% (80 °C) to  
199 79.08% (120 °C), and decreased thereafter to 76.64% (130 °C) and 38.82% (150 °C). Two  
200 reasons may explain the decreased lignin removal at high temperature: 1) repolymerization of  
201 lignin degradation products that increased the lignin content; 2) the generation of pseudo-  
202 lignin from carbohydrate degradation and condensation that precipitated back onto the surface  
203 of substrate. The decrease in delignification efficiency explained the increased solid recovery  
204 at 130 and 150 °C as shown in Fig. 1a. As well known, both the lignin repolymerization and  
205 pseudo-lignin are rich in aromatic structure which is more hydrophobic than natural lignin and  
206 thus has stronger inhibition on enzymatic hydrolysis. This result indicated that 120 °C is the  
207 optimal pretreatment temperature in terms of delignification efficiency, while higher  
208 temperature might contribute to lignin repolymerization and formation of pseudo lignin thus  
209 increasing the lignin content (He et al., 2020; Hu et al., 2012). In other studies, Wang et al.

210 reported that ChCl/p-hydroxybenzoic acid (PB) has a 69.00% delignification at 160 °C for 3 h  
211 (Wang et al., 2020). For the most famous ChCl/lactic acid system, only 58.20% delignification  
212 was achieved at even 145 °C for 3 h (Alvarez-Vasco, 2016). Compared to other organic  
213 solvents, such as valerolactone, isopropanol and propylene carbonate, our guaiacol-DES was  
214 also advantageous in the aspects of low temperature, short pretreatment time and high  
215 recyclability (Dutta et al., 2022).

### 216 3.2. Morphology of the pretreated samples

217 The effect of the guaiacol-based pretreatment on biomass can be clearly evidenced by the  
218 color changes of the pretreated samples (see Supplementary materials). The raw bamboo was  
219 in somehow light brown color, which turned into brown at mild temperatures (80-100 °C) and  
220 finally became almost black at higher temperatures (higher than 110 °C). This might be caused  
221 by the mitigation of dissolved lignin from the inner part to the out surface of the pretreated  
222 biomass. In addition, the caramelization of the dissolved sugar (mainly derived from xylan  
223 degradation) and the formation of pseudo-lignin also favored the darkening of the high-  
224 temperature pretreated samples, especially at 150 °C (Nitsos et al., 2019). Similar color  
225 changes were also observed for the DES-treated samples with various AlCl<sub>3</sub> loadings and  
226 different ChCl to guaiacol ratios. Specifically, the color of the pretreated sample remained  
227 light brown without the addition of AlCl<sub>3</sub>, while the color of pretreated materials darkened as  
228 more AlCl<sub>3</sub> was used, which revealed that the lignin migration/degradation was enhanced at  
229 higher AlCl<sub>3</sub> dosage. This is because that the H-bond between guaiacol and ChCl was  
230 enhanced with the introduction of AlCl<sub>3</sub> which as a result reinforced the H-bond between

231 guaiacol and bamboo, and caused its fractionation. However, it was also found that the color of  
232 pretreated materials became light with the increase of the ChCl to guaiacol ratio while  
233 maintaining the same ChCl to AlCl<sub>3</sub> molar ratio, indicating that increase of guaiacol usage  
234 benefitted the pretreatment.

235 The morphological discrepancy of all the pretreated sample was evaluated by SEM (see  
236 [Supplementary materials](#)). The raw bamboo sample is a class of long fibers with smooth  
237 surface texture, and rigid and compact structure, which could hinder the access of the cellulase  
238 to cellulose. In contrast, the size of the DES-treated samples was apparently reduced, and some  
239 small cracks could be detected on the surface of the fibers. Further temperature enhancement  
240 (especially higher than 110 °C) aggregated short bamboo fibers and formed many visible  
241 agglomerates. This is because of the significant removal of hemicellulose and lignin that  
242 exposed the cellulose and contributed to the formation of hydrogen bonds between the  
243 cellulose-enriched fibers. Besides, the surface of the fiber at high temperatures (higher than  
244 100 °C) shrunk due to lignin/hemicellulose degradation, and a wrinkled surface texture  
245 appeared on the surface, which increased the accessible surface area of cellulose. In addition,  
246 at a very high temperature (especially 150 °C), small lignin flakes were deposited on the fiber  
247 surface (see inset), which is caused by the formation of large pseudo-lignin moieties that could  
248 not be removed with repeated acetone/water washing. These lignin flakes could be negatively  
249 adsorbed by the enzymes and consequently decrease the enzymatic hydrolysis yield and rate.

250 3.3. Chemical structure analysis

251 The effects of the proposed DES pretreatment on the biomass CrI and cellulose DP of the  
252 pretreated sample were further investigated, and results are shown in Fig. 2. The raw moso  
253 bamboo has a CrI of 62.02%, slightly higher than that of poplar, wheat, and other bamboo  
254 species (Ling et al., 2020; Wang et al., 2020). With the increase of the temperature, the CrI  
255 increased gradually and finally reached the maximum of 66.96% at 110 °C. The increase of  
256 biomass CrI can be due to the removal of amorphous lignin and hemicellulose. However, CrI  
257 started to decrease as the pretreatment temperature increased to 120 °C (66.17%) and 130 °C  
258 (65.99%), which might be caused by the penetration of guaiacol-DES into the crystalline  
259 portion of cellulose at higher temperatures. Furthermore, the CrI was dramatically reduced to  
260 57.68% at 150 °C, which could be due to the formation of amorphous pseudo-lignin at such a  
261 high temperature (see Supplementary material).

262 To better understand the cellulose structure changes during the DES pretreatment, the  $\alpha$ -  
263 cellulose in the pretreated samples was isolated and used for the DP analysis. It can be seen in  
264 Fig. 2b that the DP of the raw moso bamboo was 1106, indicating a relative long fiber length  
265 (Cheng et al., 2019). With the increase of the temperature, cellulose DP decreased accordingly  
266 to 1057 (80 °C), 702 (90 °C), 601 (100 °C), and 492 (110 °C). In consideration of the high  
267 glucan recovery during the pretreatment (Fig. 1), it can be concluded that the guaiacol DES  
268 cleaved the long cellulose chain into shorter ones rather than degrading it, which may expose  
269 more reducing ends and thus increase the accessibility of the pretreated bamboo cellulose.  
270 Further increasing the temperature (110-150 °C) had a very limited impact on the cellulose DP.

271 FTIR spectra of the raw and pretreated samples were performed to reveal the variations of  
272 the chemical structure (see Supplementary material). The peaks were assigned according to the  
273 previous literature (Yoo et al., 2017). It can be seen that the peak for hydroxyl groups at 3337  
274  $\text{cm}^{-1}$  was enhanced after the DES pretreatment. This result indicated an increased hydroxyl  
275 groups with the removal of hydrophobic lignin. Signals for the hemicellulose (C=O ester in  
276 LCC (lignin-carbohydrate complex) and carbonyl groups) at 1730  $\text{cm}^{-1}$  gradually diminished  
277 as increasing the temperature and it finally disappeared at 130 °C, revealing the significant  
278 hemicellulose degradation. However, this signal was observed again at the temperature of  
279 150 °C. Other researchers also reported the same phenomenon in the hydrothermal  
280 pretreatment, and the authors ascribed it to the formation of the Hibbert ketones induced by the  
281 cleavage of aryl ether bonds in lignin (Nitsos et al., 2019). In addition, signals at 1602  $\text{cm}^{-1}$  and  
282 1507  $\text{cm}^{-1}$ , attributed to the lignin skeleton stretching and vibration was decreased, which  
283 indicated the strong delignification by the guaiacol DES. Strikingly, the signals at 1318  $\text{cm}^{-1}$   
284 (C-O vibrations of syringyl unit) increased after the pretreatment, while that for syringyl unit  
285 (C-O vibration) decreased, this result suggested that the proposed DES favored to degrade the  
286 G unit in lignin. In case of the cellulose signals (C-H deformation at 1422  $\text{cm}^{-1}$ , C-H stretching  
287 at 1367  $\text{cm}^{-1}$ , C-O-C asymmetrical stretching at 1158  $\text{cm}^{-1}$ , C-O vibration at 1101  $\text{cm}^{-1}$  and  $\beta$ -  
288 glycosidic linkage at 896  $\text{cm}^{-1}$ ), they became strengthened as increasing the temperature until  
289 110 °C and then decreased due to the reduce in cellulose content by the formation of pseudo-  
290 lignin.

291 3.4. Enzymatic hydrolysis

292 Enzymatic hydrolysis (EH) is the key step for converting glucan into glucose, and the EH  
293 yield of the guaiacol DES pretreated samples is shown in Fig. 3. The EH yield for raw moso  
294 bamboo was less than 10% (both for glucan and xylan, data not shown). After the DES  
295 pretreatment, glucan hydrolysis yield increased gradually from 14.31% to 35.60%, 69.28%,  
296 and 96.20% as the temperature increased from 80 to 90, 100, 110°C, respectively. Finally, a  
297 near 100% cellulose conversion was observed for pretreated bamboo at 120 °C. Xylan  
298 hydrolysis yield followed a similar trend in this study. It should be noted that xylan hydrolysis  
299 yield at high temperatures was not reported due to the fact that only trace amount of xylan left  
300 in the pretreated residue. It can be seen that the enzymatic hydrolysis efficiency is superior to  
301 traditional acidic or natural DES pretreatment (such as ChCl/lactic acid and ChCl/glycerol),  
302 which normally need severe conditions (e.g., high temperature or long pretreatment time) to  
303 boost the cellulose conversion (Shen et al., 2019). Furthermore, glucan hydrolysis yield  
304 sharply decreased to 63.08% and 58.86% when the pretreatment temperature increased to 130  
305 and 150 °C. Interestingly, pretreated samples at 120 and 130 °C had very similar lignin content  
306 (Fig. 1), however, the cellulose hydrolysis yield of pretreated bamboos at 130 °C is  
307 significantly lower (36.92% decrease) than that of the pretreated sample at 120 °C. To further  
308 evaluate the effect of individual components (e.g., xylan and lignin) on the EH of cellulose,  
309 glucan hydrolysis yield was plotted against the removal of xylan and lignin (Fig. 4). Overall,  
310 the enzymatic digestibility showed a positive relationship with xylan removal and lignin  
311 removal, which indicated that both the solubilization of xylan and lignin induced by the  
312 guaiacol DES favored the enzymatic hydrolysis. In other studies, strong association between

313 EH yield and lignin removal was normally observed, while its correlation with xylan removal  
314 was not that obvious (Meng et al., 2015; Sun et al., 2016). Furthermore, when removing the  
315 samples at 130 and 150 °C (insets in Fig. 4), a strong correlation between EH yield and xylan  
316 and lignin removal was observed, with a  $R^2$  values of 0.99 and 0.98, respectively. These results  
317 indicated that during the DES pretreatment, the quantity of xylan and lignin in some extent  
318 governs the enzymatic hydrolysis, while at high temperatures, other factors, such as lignin  
319 hydrophobicity, degree of lignin condensation, and molecular weight, might play a more  
320 important role.

321 The effect of ChCl to guaiacol molar ratio on the enzymatic hydrolysis efficiency was  
322 also evaluated (see Supplementary materials). At the molar ratio of 1:1, it cannot form a  
323 homogeneous liquid and thus this combination was excluded from the investigation. As the  
324 molar ratio of ChCl to guaiacol decreased, a transparent and clear DES was formed due to the  
325 abundance of H bonds between the HBA and HBD. It was found that the EH yield  
326 considerably decreased from 100% to 92.27% and 76.68% as the ChCl to guaiacol molar ratio  
327 decreased from 1:2 to 1:5. This was probably due to the decreased active acidic sites of the  
328 DES as a result of decreasing the HBA to HBD molar ratio. The effect of  $AlCl_3$  dosage during  
329 the DES pretreatment on the EH yield was also investigated (see Supplementary materials). It  
330 was found that  $AlCl_3$  played an essential role in the DES pretreatment as indicated by the  
331 extremely low glucan hydrolysis yield in the absence of  $AlCl_3$ . While with only a minor  
332 addition of  $AlCl_3$  (molar ratio of 25:50:0.2), the EH yield significantly increased to 68.37%.  
333 The EH yield further increased to 71.70%, 86.05% and 96.20% at the ChCl:guaiacol: $AlCl_3$  of

334 25:50:0.4, 25:50:0.8, 25:50:1, respectively. This result indicated that the addition of  $\text{AlCl}_3$   
335 promoted the fractionation efficiency, and increased the enzymatic digestibility.

### 336 3.4 Characterization of regenerated lignin

337 The molecular weight ( $M_w$  and  $M_n$ ) and dispersity ( $\mathcal{D}$ ) of the regenerated lignins were  
338 measured by GPC, and the results are shown in Table 1. The molecular weight of the raw  
339 bamboo CEL was 12322 and 3656 g/mol for  $M_w$  and  $M_n$ , respectively. After the DES  
340 pretreatment, the regenerated lignins possessed a much lower molecular weight. Even at  
341 80 °C, the  $M_w$  decreased to 2986 g/mol. As widely reported in literature, lignin typically  
342 suffered from both degradation and condensation during acid-catalyzed biomass pretreatment.  
343 The decrease in the  $M_w$  implied a significant lignin depolymerization during the DES  
344 pretreatment. With the increase of temperature to higher values (100-120 °C), the  $M_w$  of lignin  
345 slightly increased, which may be caused by the lignin condensation at these temperatures.  
346 However, a further increase of the pretreatment temperature to 130 °C largely decreased the  
347 lignin  $M_w$  back to 2186 g/mol. This result indicated that lignin degradation was faster than its  
348 condensation at high DES pretreatment severity. In addition, the  $\mathcal{D}$  of the regenerated lignins  
349 decreased after all the DES pretreatment.

350 Lignin valorization potential strongly depends on its chemical structure. In this study, the  
351 chemical structure of the raw bamboo CEL and the regenerated lignins was analyzed with 2D  
352 HSQC NMR (see Supplementary materials). The assignments of the NMR spectra cross  
353 signals were referred to previous literature (Wang et al., 2020). In the aromatic regions ( $\delta_C/\delta_H$   
354 100.0-150.0/6.0-8.1 ppm), raw bamboo CEL showed clear signals for syringyl ( $S_{2/6}$ ), guaiacyl

355 (G<sub>2</sub>, G<sub>5</sub>, G<sub>6</sub>), and *p*-hydroxyphenyl (H<sub>2/6</sub>) units, with the content of 42.19%, 46.75% and  
356 11.05%, respectively (Table 2). In addition, a small amount of oxidized S unit (S'<sub>2/6</sub>) was also  
357 detected. Besides, large *p*-coumarate (24.90%, PCE<sub>2/6</sub>, PCE<sub>7</sub>, and PCE<sub>8</sub>) signals as well as  
358 small ferulate (11.09%, FA<sub>2</sub>, FA<sub>6</sub>, and FA<sub>7</sub>) signals were observed in CEL, attributing to the  
359 high content of lignin-carbohydrates complex in bamboo. The signals associated with triclin  
360 (T<sub>3</sub>) also existed in the raw bamboo CEL which have been also reported in other types of  
361 herbaceous plants (Li et al., 2016). In the regenerated DES lignin, signals arising from S' and  
362 T were all weakened and finally disappeared at the temperature higher than 110 °C, while the  
363 PCE peaks were all well preserved even at those high temperatures. Noticeably, significant  
364 lignin condensations were observed in all the DES lignin samples even at a mild pretreatment  
365 temperature such as 90 °C. As expected, the correlated signals of the condensed structure were  
366 intensified as the temperature increased from 90 to 130 °C. In the regenerated lignin, the S/G  
367 ratio significantly decreased after DES pretreatment. One possible explanation for the  
368 decreased S/G ratio is the demethoxylation of S unit during the pretreatment, thus leading to  
369 the formation of more G-type units (Wen et al., 2015). This conjecture could also explain the  
370 increased H unit content (1.83% to 5.02% as temperature from 90 to 130 °C) after the DES  
371 pretreatment.

372 In the side-chain region ( $\delta_C/\delta_H$  50.0-90.0/2.0-6.1 ppm), strong signals of  $\beta$ -O-4 (A) in  
373 CEL was obviously identified, along with the weak signals from  $\beta$ - $\beta$  (B) and  $\beta$ -5 (C), whose  
374 contents were 57.75%, 5.86% and 7.45% (Table 2), respectively. In addition,  $\gamma$ -acylated A unit  
375 was also observed, indicating the existence of LCC structure. In the regenerated DES lignin,

376 the interunit linkages especially the aryl ether linkages suffered from a significant cleavage  
377 even at 90 °C (*i.e.*, ~87% decrease), indicating significant lignin depolymerization during the  
378 DES pretreatment. It should be noted that the carbohydrate signals, which could be clearly  
379 seen in raw bamboo CEL, was only detected at a noise level in these regenerated DES lignin  
380 substrates, revealing its high purity. With increasing temperature, these interlinkages signals  
381 continued decreasing, and finally no  $\beta$ -O-4 structure was observed at temperature  $\geq 110$  °C,  
382 which agreed with other report showing that  $\beta$ -O-4 linkage is quite vulnerable at the acidic  
383 condition (Wang et al., 2019). Overall, the guaiacol-DES showed high delignification ability in  
384 which the lignin can be used in the downstream thermochemical depolymerization to generate  
385 guaiacol, thus contributing to the establishment of a renewable and sustainable biorefinery  
386 sequence.

### 387 3.5 DES recovery and reuse

388 Compared to other solvents, DES is advantageous in the aspect of its high recyclability as  
389 it can be recovered by simply removing the antisolvent that was used to recovery lignin. In this  
390 study, the guaiacol-based DES was recycled at the end of the first run and was tested for its  
391 reusing ability to pretreat bamboo multiple times at the temperature of 120 °C. The DES  
392 recovery and delignification efficiency were analyzed. In each cycle, more than 90% of DES  
393 (data now shown) could be recovered and reused for the next round pretreatment. During those  
394 runs, the solid recovery increased from 53.12% to 73.19%, 80.42%, and 80.50% for  
395 pretreatment cycle 2, 3, and 4, respectively (Fig. 5), showing an obvious reduction in  
396 pretreatment efficiency. Similar to the solid recovery, the lignin removal decreased

397 significantly from 79.08% to 38.77%, 30.30%, and 30.17%, accompanied by a reduced EH  
398 yield from 100% to 51.66%, 28.18%, and 24.88% accordingly. Two reasons may explain the  
399 lowered DES pretreatment efficiency: (1) consumption of the  $\text{AlCl}_3$  during the pretreatment  
400 that weakened the acidic strength and the hydrogen-bond interaction of the DES; (2) the  
401 impurities from lignin/hemicellulose degradation that contaminated the DES and lowered its  
402 efficiency (Chen et al., 2018). To test these hypotheses, additional  $\text{AlCl}_3$  (with amount equal to  
403 that in the initial DES) was supplemented into the recovered DES, which clearly boosted the  
404 lignin removal (Fig. 5a). It should be noted that the lignin removal was still lower than the  
405 fresh DES, indicating that the impurities, especially the accumulated products from  
406 hemicellulose depolymerization, might hinder the DES pretreatment. With the supplement of  
407  $\text{AlCl}_3$ , the glucan EH yields were 90.68%, 83.07%, and 72.30% in the recycled DES  
408 pretreatment, which proved that DES is a low-cost and recyclable green solvent for bamboo  
409 fractionation.

### 410 3.6 Mechanism of the $\text{AlCl}_3$ induced DES fractionation

411 From the above results, the  $\text{AlCl}_3$  played a key role in the guaiacol-based DES  
412 pretreatment, and a possible mechanism of the guaiacol DES was proposed in this section. It is  
413 well known that choline cation is a tetrahedron composed of the methyl and methylene groups  
414 of a quaternary ammonium with  $\text{CH}_2\text{OH}$  extended, which endows the capability to form H-  
415 bond with the hydroxyl groups in the guaiacol. In the  $\text{ChCl}$ /guaiacol system, the main H bond  
416 was formed between choline and hydroxyl groups (in guaiacol) with respect to the N-C-C-O  
417 torsion angle, and the H bond between Cl and hydroxyl groups was deemed to be very weak

418 due to the low electron density of Cl (Yu et al., 2019a). As a combination, the interaction  
419 between the ChCl and guaiacol interfered with the initial compositions of the mixture to  
420 crystallize and lead to the formation of a homogeneous liquid. However, due to the weak  
421 proton donating ability (weak acidity) of guaiacol, the hydrogen bond between ChCl and  
422 guaiacol is relatively weak, thus the H bond between choline and guaiacol is not stronger than  
423 that of other organic acid (such as lactic acid), and the residual phenolic-O: exhibited low  
424 affinity to form the H bond with the biomass, resulting in poor delignification of the DES. In  
425 the case of the three-constituent ChCl/guaiacol/ $\text{AlCl}_3$  DES system, Al can coordinate with  
426 guaiacol through electron-abundant O in phenolic hydroxyl groups and contribute to the  
427 formation of an unidentate ligand (Yu et al., 2019b). In this system, Al competes with choline  
428 to attract the O of phenolic groups. As a result of the coordination reaction, the polarity of the  
429 phenolic hydroxyl groups increased, which promoted the H bond between guaiacol and choline  
430 and reinforced the H bond between guaiacol and biomass. In addition, the increased acidity by  
431  $\text{AlCl}_3$  addition enhanced the cleavage of aryl ether during the pretreatment and caused high  
432 lignin removal. Overall, the ternary system seems to be a supramolecule in which guaiacol is  
433 in somewhat like a bride, and Al attract the electron of O, thus enhancing the acidity of the  
434 solvent and facilitating its fractionation efficiency (Xia et al., 2018).

#### 435 **4. Conclusion**

436 The guaiacol DES showed excellent performance in removing xylan (>90%) and lignin  
437 (as high as 79.1%) at mild temperatures. After pretreatment, cellulose DP was significantly  
438 decreased, but the CrI showed a crescent trend, which overall enhanced the enzymatic

439 digestibility of the substrates. Lignin suffered from serious degradation and condensation  
440 reactions during the pretreatment with the aryl ether interlinkage being severely cleaved. The  
441 role of AlCl<sub>3</sub> in enhancing the efficacy was analyzed, which revealed the mechanism of the  
442 guaiacol-DES in fractionating biomass and improving the enzymatic hydrolysis.

443 E-supplementary data for this work can be found in e-version of this paper online

#### 444 **Notes**

445 The authors declare no competing financial interest.

#### 446 **Acknowledgmentsxr**

447 This research was supported by Jiangsu Province Key Laboratory of Biomass  
448 Engineering and Materials (JSBEM-S-202203, JSBEM-S-202004), Guangxi Key Laboratory  
449 of Clean Pulp & Papermaking and Pollution Control, College of Light Industry and Food  
450 Engineering, Guangxi University (2021KF34) and Taishan Industrial Experts Programme  
451 (tscy20200213). AJR efforts were supported by University of Tennessee, Knoxville.

#### 452 **Reference:**

- 453 1. Alayont, Ş., Kayan, D.B., Durak, H., Alayont, E.K., Genel, S. 2022. The role of acidic, alkaline  
454 and hydrothermal pretreatment on pyrolysis of wild mustard (*Sinapis arvensis*) on the  
455 properties of bio-oil and bio-char. *Bioresource Technology Reports*, **17**, 100980.
- 456 2. Alvarez-Vasco, C.M., R; Quintero, M; Guo, M; Geleynse, S; Ramasamy, K; Wolcott, M; Zhang, X.  
457 2016. Unique Low-molecular-weight Lignin with High Purity Extracted from Wood\_\_by  
458 Deep Eutectic Solvents (DES): A Source of Lignin for Valorization. *Green Chemistry*, **18**,  
459 5133-5141.

- 460 3. Bueren, J.B.D., Héroguel, F., Wegmann, C., Dick, G.R., Buser, R., Luterbacher, J.S. 2020.  
461 Aldehyde-Assisted Fractionation Enhances Lignin Valorization in Endocarp Waste Biomass.  
462 *ACS Sustainable Chemistry & Engineering*, **8**(45), 16737-16745.
- 463 4. Buzala, K.P., Kalinowska, H., Przybysz, P., Malachowska, E. 2017. Conversion of various types of  
464 lignocellulosic biomass to fermentable sugars using kraft pulping and enzymatic hydrolysis.  
465 *Wood Science and Technology*, **51**(4), 873-885.
- 466 5. Carvalho, D.M.d., Queiroz, J.H.d., Colodette, J.L. 2016. Assessment of alkaline pretreatment for  
467 the production of bioethanol from eucalyptus, sugarcane bagasse and sugarcane straw.  
468 *Industrial Crops and Products*, **94**, 932-941.
- 469 6. Chen, Z., Reznicek, W.D., Wan, C. 2018. Aqueous Choline Chloride: A Novel Solvent for  
470 Switchgrass Fractionation and Subsequent Hemicellulose Conversion into Furfural. *ACS*  
471 *Sustainable Chemistry & Engineering*, **6**(5), 6910-6919.
- 472 7. Cheng, J., Huang, C., Zhan, Y., Han, S., Wang, J., Meng, X., Yoo, C.G., Fang, G., Ragauskas, A.J.  
473 2022. Effective biomass fractionation and lignin stabilization using a diol DES system.  
474 *Chemical Engineering Journal*, **443**, 136395.
- 475 8. Cheng, L., Wang, L., Wei, L., Wu, Y., Alam, A., Xu, C., Wang, Y., Tu, Y., Peng, L., Xia, T. 2019.  
476 Combined mild chemical pretreatments for complete cadmium release and cellulosic  
477 ethanol co-production distinctive in wheat mutant straw. *Green Chemistry*, **21**(13), 3693-  
478 3700.
- 479 9. Dutta, S., Yu, I.K.M., Fan, J., Clark, J.H., Tsang, D.C.W. 2022. Critical factors for levulinic acid  
480 production from starch-rich food waste solvent effects, reaction pressure, and phase

- 481 separation. *Green Chemistry*, **24**, 163-175.
- 482 10. He, J., Huang, C., Lai, C., Huang, C., Li, M., Pu, Y., Ragauskas, A.J., Yong, Q. 2020. The effect of  
483 lignin degradation products on the generation of pseudo-lignin during dilute acid  
484 pretreatment. *Industrial Crops and Products*, **146**, 112205.
- 485 11. Ho, M.C., Ong, V.Z., Wu, T.Y. 2019. Potential use of alkaline hydrogen peroxide in lignocellulosic  
486 biomass pretreatment and valorization – A review. *Renewable and Sustainable Energy  
487 Reviews*, **112**, 75-86.
- 488 12. Hu, F., Jung, S., Ragauskas, A. 2012. Pseudo-lignin formation and its impact on enzymatic  
489 hydrolysis. *Bioresource Technology*, **117**, 7-12.
- 490 13. Huang, C., Zhan, Y., Cheng, J., Wang, J., Meng, X., Zhou, X., Fang, G., Ragauskas, A.J. 2021.  
491 Facilitating enzymatic hydrolysis with a novel guaiacol-based deep eutectic solvent  
492 pretreatment. *Bioresour Technol*, **326**, 124696.
- 493 14. Huang, C., Zhan, Y., Wang, J., Cheng, J., Meng, X., Liang, L., Liang, F., Deng, Y., Fang, G.,  
494 Ragauskas, A.J. 2022. Valorization of bamboo biomass using combinatorial pretreatments.  
495 *Green Chemistry*.
- 496 15. Li, M., Pu, Y., Yoo, C.G., Ragauskas, A.J. 2016. The occurrence of triclin and its derivatives in  
497 plants. *Green Chemistry*, **18**(6), 1439-1454.
- 498 16. Ling, Z., Guo, Z., Huang, C., Yao, L., Xu, F. 2020. Deconstruction of oriented crystalline cellulose  
499 by novel levulinic acid based deep eutectic solvents pretreatment for improved enzymatic  
500 accessibility. *Bioresource Technology*, **305**, 123025.
- 501 17. Liu, Z.-H., Hao, N., Shinde, S., Pu, Y., Kang, X., Ragauskas, A.J., Yuan, J.S. 2019. Defining lignin

502 nanoparticle properties through tailored lignin reactivity by sequential organosolv  
503 fragmentation approach (SOFA). *Green Chemistry*, **21**(2), 245-260.

504 18. Meng, X., Pu, Y., Sannigrahi, P., Li, M., Cao, S., Ragauskas, A.J. 2017. The Nature of Hololignin.  
505 *ACS Sustainable Chemistry & Engineering*, **6**(1), 957-964.

506 19. Meng, X., Wells, T., Sun, Q., Huang, F., Ragauskas, A. 2015. Insights into the effect of dilute  
507 acid, hot water or alkaline pretreatment on the cellulose accessible surface area and the  
508 overall porosity of Populus. *Green Chemistry*, **17**(8), 4239-4246.

509 20. Nitsos, C.K., Lazaridis, P.A., Mach-Aigner, A., Matis, K.A., Triantafyllidis, K.S. 2019. Enhancing  
510 Lignocellulosic Biomass Hydrolysis by Hydrothermal Pretreatment, Extraction of Surface  
511 Lignin, Wet Milling and Production of Cellulolytic Enzymes. *ChemSusChem*, **12**(6), 1179-  
512 1195.

513 21. Pielhop, T., Larrazábal, G.O., Studer, M.H., Brethauer, S., Seidel, C.-M., Rudolf von Rohr, P.  
514 2015. Lignin repolymerisation in spruce autohydrolysis pretreatment increases cellulase  
515 deactivation. *Green Chemistry*, **17**(6), 3521-3532.

516 22. Ragauskas, A.J.W., C. K.; Davison, B. H.; Britovsek, G.; Cairney, J.E., C. A.; Frederick, W. J., Jr.;  
517 Hallett, J. P.; Leak, D., J.; Liotta, C.L.M., J. R.; Murphy, R.; Templer, R.; Tschaplinski, T, T.  
518 2006. The path forward for biofuels and biomaterials. *Science*, **311**, 484-489.

519 23. Shen, X., Meng, Q., Mei, Q., Liu, H., Yan, J., Song, J., Tan, D., Chen, B., Zhang, Z., Yang, G., Han,  
520 B. 2020. Selective catalytic transformation of lignin with guaiacol as the only liquid product.  
521 *Chemical Science*, **11**(5), 1347-1352.

522 24. Shen, X.-J., Wen, J.-L., Mei, Q.-Q., Chen, X., Sun, D., Yuan, T.-Q., Sun, R.-C. 2019. Facile

523 fractionation of lignocelluloses by biomass-derived deep eutectic solvent (DES)  
524 pretreatment for cellulose enzymatic hydrolysis and lignin valorization. *Green Chemistry*,  
525 **21**(2), 275-283.

526 25. Shuai, L.A., T., Masoud; Questell-Santiago, M., Ydna; Héroguel, Florent;, Li, Y.K., Hoon; Meilan,  
527 Richard; Chapple, Clint;, Ralph, J.L., S., Jeremy. 2016. Formaldehyde stabilization facilitates  
528 lignin monomer production during biomass depolymerization. *Science*, **354**(6310), 329-333.

529 26. Sluiter, A., Hames, B., Ruiz, R., Scarlata, C., Sluiter, J., Templeton, D. 2008. Laboratory Analytical  
530 Procedure (LAP). *Technical Report, 2008*.

531 27. Studer, M.H., DeMartini, J. D., , Davis, M.F., Sykes, R.W., Davison, B., Keller, M., Tuskan, G.A.,  
532 Wyman, C.E. 2011. Lignin content in natural *Populus* variants affects sugar release. *PNAS*,  
533 **108**, 6300-6305.

534 28. Sun, S., Huang, Y., Sun, R., Tu, M. 2016. Strong association of condensed phenolic moieties in  
535 isolated\_\_lignins with their inhibition of enzymatic hydrolysis. *Green Chemistry*, **18**, 4276-  
536 4286.

537 29. Wang, Y., Meng, X., Jeong, K., Li, S., Leem, G., Kim, K.H., Pu, Y., Ragauskas, A.J., Yoo, C.G.  
538 2020. Investigation of a Lignin-Based Deep Eutectic Solvent Using p-Hydroxybenzoic Acid  
539 for Efficient Woody Biomass Conversion. *ACS Sustainable Chemistry & Engineering*, **8**(33),  
540 12542-12553.

541 30. Wang, Z.-K., Hong, S., Wen, J.-l., Ma, C.-Y., Tang, L., Jiang, H., Chen, J.-J., Li, S., Shen, X.-J.,  
542 Yuan, T.-Q. 2019. Lewis Acid-Facilitated Deep Eutectic Solvent (DES) Pretreatment for  
543 Producing High-Purity and Antioxidative Lignin. *ACS Sustainable Chemistry & Engineering*,

544           **8**(2), 1050-1057.

545   31. Wen, J.-L., Sun, S.-L., Xue, B.-L., Sun, R.-C. 2015. Structural elucidation of inhomogeneous  
546           lignins from bamboo. *International Journal of Biological Macromolecules*, **77**, 250-259.

547   32. Xia, Q., Liu, Y., Meng, J., Cheng, W., Chen, W., Liu, S., Liu, Y., Li, J., Yu, H. 2018. Multiple  
548           hydrogen bond coordination in three-constituent deep eutectic solvents enhances lignin  
549           fractionation from biomass. *Green Chemistry*, **20**(12), 2711-2721.

550   33. Yoo, C.G., Li, M., Meng, X., Pu, Y., Ragauskas, A.J. 2017. Effects of organosolv and ammonia  
551           pretreatments on lignin properties and its inhibition for enzymatic hydrolysis. *Green*  
552           *Chemistry*, **19**(8), 2006-2016.

553   34. Yu, I.K.M., Tsang, D.C.W., Yip, A.C.K., Su, Z., Vigier, K., D.O., Jérôme, F., Poon, C., S., Ok, Y.S.  
554           2019a. Organic Acid-Regulated Lewis Acidity for Selective\_\_Catalytic  
555           Hydroxymethylfurfural Production from Rice Waste: An Experimental-Computational Study.  
556           *ACS Sustainable Chemistry & Engineering*, **7**(1), 1437-1446.

557   35. Yu, I.K.M., Xiong, X., Tsang, D.C.W., Wang, L., Hunt, A.J., Song, H., Shang, J., Ok, Y.S., Poon, C.S.  
558           2019b. Aluminium-biochar composites as sustainable heterogeneous catalysts for glucose  
559           isomerisation in a biorefinery. *Green Chemistry*, **21**(6), 1267-1281.

560   36. Zhan, Y., Cheng, J., Liu, X., Huang, C., Wang, J., Han, S., Fang, G., Meng, X., Ragauskas, A.J.  
561           2022. Assessing the availability of two bamboo species for fermentable sugars by alkaline  
562           hydrogen peroxide pretreatment. *Bioresour Technol*, **349**, 126854.

563

565 **Figures legends**

566 **Fig. 1.** Solid (a) and composition (b) recoveries during the guaiacol-DES at elevated  
567 temperatures.

568 **Fig. 2.** Biomass CrI (a) and cellulose DP (b) analysis of the untreated and pretreated samples.

569 **Fig. 3.** Enzymatic hydrolysis yield of the pretreated samples.

570 **Fig. 4.** Correlation between enzymatic hydrolysis yield and the removal of xylan (a) and lignin  
571 (b).

572 **Fig. 5.** Composition recovery (a) and enzymatic hydrolysis (b) during the DES recycling.

573

574

575

576

577

578

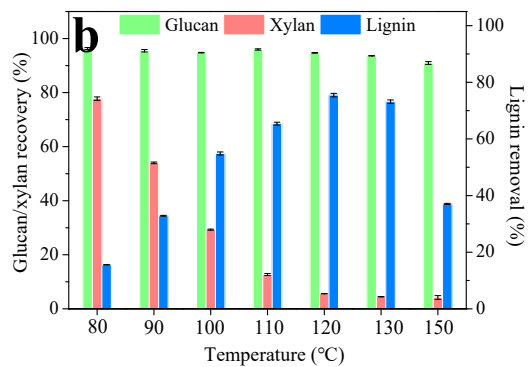
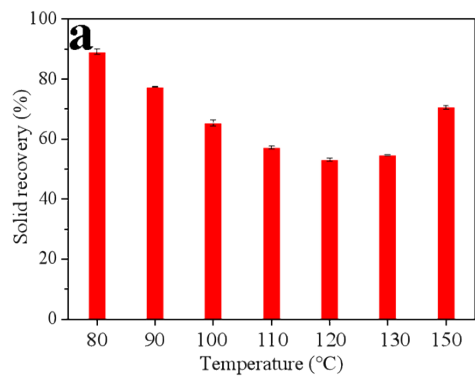
579

580

581

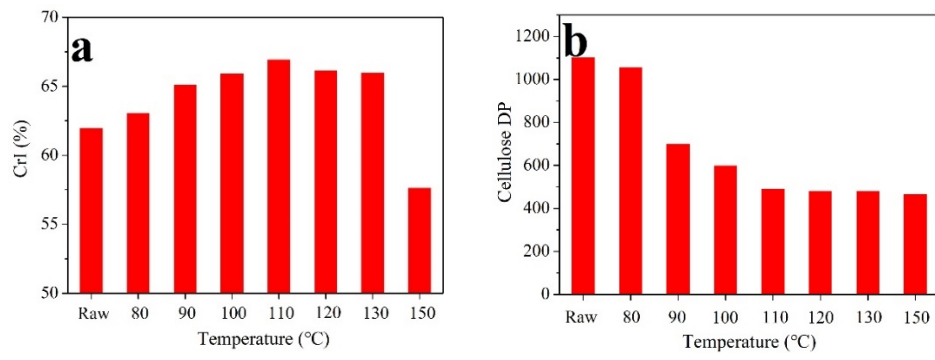
582

583



584  
585 **Fig. 1.**  
586

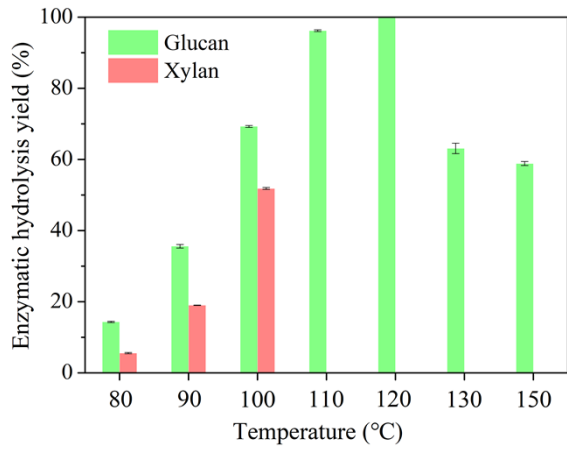
587



588

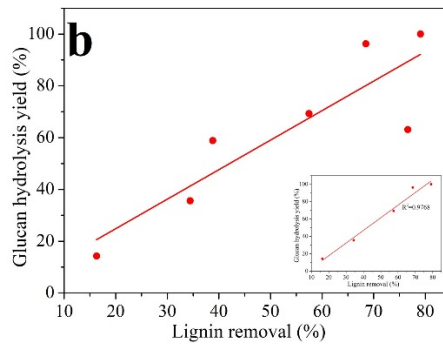
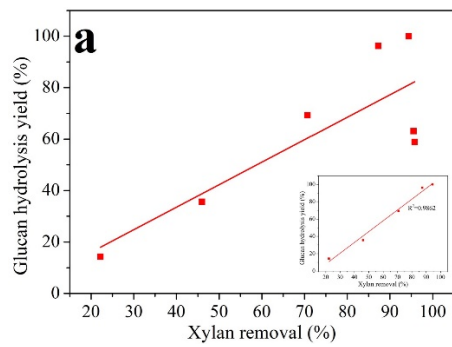
589 **Fig. 2.**

590



591

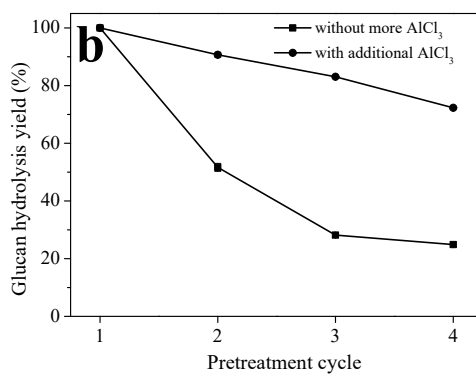
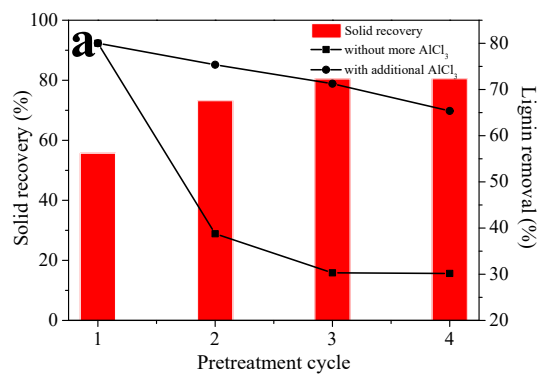
592 **Fig. 3.**



594  
595 **Fig. 4.**

596

597



598

599 **Fig. 5.**

600

601 **Table 1** Weight-average ( $M_w$ ) and number-average ( $M_n$ ) molecular weights, and dispersity ( $\mathcal{D}$ )  
602 of the regenerated lignins.

Sample	$M_w$ (g/mol)	$M_n$ (g/mol)	$\mathcal{D}$
Bamboo CEL	12322	3656	3.37
DES 80°C	2986	1267	2.36
DES 90°C	2797	1295	2.16
DES 100°C	3154	1540	2.05
DES 110°C	3105	1289	2.41
DES 120°C	3295	1300	2.53
DES 130°C	2186	1070	2.04

603

605 **Table 2** Semiquantitative data of aromatic units and the content of interunit linkages.

	CEL	90 °C	100 °C	110 °C	120 °C	130 °C
<b>Lignin subunits (%)</b>						
S	42.19	35.65	33.25	24.46	23.78	23.20
G	46.75	62.52	62.23	70.96	71.65	71.78
H	11.05	1.83	4.52	4.57	4.56	5.02
S/G	0.90	0.57	0.53	0.34	0.33	0.32
<b>End groups (%)</b>						
Ferulic acid	11.09	0.00	0.00	0.00	0.00	0.00
p-Coumaric acid	24.90	19.62	14.08	8.77	9.17	12.88
<b>Interunit linkages (%)</b>						
$\beta$ -O-4	57.75	7.42	2.09	0.00	0.00	0.00
$\beta$ - $\beta$	5.86	2.24	1.69	0.97	0.91	0.66
$\beta$ -5	7.46	1.66	0.86	0.10	0.00	0.00

606